J Ginseng Res 44 (2020) 413–423

Contents lists available at ScienceDirect

Journal of Ginseng Research

journal homepage: http://www.ginsengres.org

Research Article

Unraveling dynamic metabolomes underlying different maturation stages of berries harvested from *Panax ginseng*

Mee Youn Lee [1], Han Sol Seo [1], Digar Singh [1], Sang Jun Lee [2], Choong Hwan Lee [1,*]

[1] *Department of Bioscience and Biotechnology, Konkuk University, Seoul, Republic of Korea*
[2] *Holistic Bio Co., Seongnam, Republic of Korea*

ARTICLE INFO

Article history:
Received 8 February 2018
Received in Revised form
28 January 2019
Accepted 13 February 2019
Available online 20 February 2019

Keywords:
Antioxidant activity
Ginseng berry
Maturation stages
Metabolic profiling
Panax ginseng

ABSTRACT

Background: Ginseng berries (GBs) show temporal metabolic variations among different maturation stages, determining their organoleptic and functional properties.
Methods: We analyzed metabolic variations concomitant to five different maturation stages of GBs including immature green (IG), mature green (MG), partially red (PR), fully red (FR), and overmature red (OR) using mass spectrometry (MS)–based metabolomic profiling and multivariate analyses.
Results: The partial least squares discriminant analysis score plot based on gas chromatography–MS datasets highlighted metabolic disparity between preharvest (IG and MG) and harvest/postharvest (PR, FR, and OR) GB extracts along PLS1 (34.9%) with MG distinctly segregated across PLS2 (18.2%). Forty-three significantly discriminant primary metabolites were identified encompassing five developmental stages (variable importance in projection > 1.0, $p < 0.05$). Among them, most amino acids, organic acids, 5-C sugars, ethanolamines, purines, and palmitic acid were detected in preharvest GB extracts, whereas 6-C sugars, phenolic acid, and oleamide levels were distinctly higher during later maturation stages. Similarly, the partial least squares discriminant analysis based on liquid chromatography–MS datasets displayed preharvest and harvest/postharvest stages clustered across PLS1 (11.1 %); however, MG and PR were separated from IG, FR, and OR along PLS2 (5.6 %). Overall, 24 secondary metabolites were observed significantly discriminant (variable importance in projection > 1.0, $p < 0.05$), with most displaying higher relative abundance during preharvest stages excluding ginsenosides Rg1 and Re. Furthermore, we observed strong positive correlations between total flavonoid and phenolic metabolite contents in GB extracts and antioxidant activity.
Conclusion: Comprehending the dynamic metabolic variations associated with GB maturation stages rationalize their optimal harvest time per se the related agroeconomic traits.

1. Introduction

Ginseng is among the most popular medicinal herbs worldwide, and it is particularly valued in Asia and North America for its pharmacological activities, namely, anticancer, antidiabetic, neuroprotective, and restorative activities [1,2]. The various pharmacologically active compounds in ginseng include ginsenosides, alkaloids, polysaccharides, polyacetylenes, and phenolic compounds [3]. However, the ginsenosides, which are structural glycosides with a dammarane skeleton, present in ginseng are primarily responsible for its pharmacological properties [4]. These compounds are distributed in many parts of the ginseng plant, including the root, stem, leaves, flowers, seeds, and fruits [5]. However, because of the disparate spatial distribution of ginsenosides in the ginseng plant, the pharmacological activities related to the different plant parts should vary substantially [6]. Previously, the antiaging, antiinflammatory, antioxidant, antiobesity, anticancer, hypoglycemic, and atopy-alleviating effects of the ginseng berry (GB) were reported [7–10]. Recently, we have shown that GB extracts possess considerably higher antioxidant potential than the roots [11]. These findings were congruent with the reportedly higher ginsenoside content in GB extracts than that in the other ginseng plant parts [12]. However, GBs are seldom considered superior, despite being rich in bioactive and functional compounds.

Mature GBs are typically harvested after 3–4 years of plant maturation depending on the variety [12]. Initially, a small berry

* Corresponding author. Department of Bioscience and Biotechnology, Konkuk University, 120 Neungdong-ro, Gwangjin-gu, Seoul 05029, Republic of Korea.
E-mail address: chlee123@konkuk.ac.kr (C.H. Lee).

https://doi.org/10.1016/j.jgr.2019.02.002
p1226-8453 e2093-4947/$ – see front matter

develops which turns green and then red in the subsequent developmental stages. At the biomolecular level, the fruit maturation and ripening processes are genetically coordinated via a complex interplay of growth regulators, plant hormones, and dynamic metabolomes, influenced by numerous biological and environmental factors [13]. Metabolite alterations in plants play an instrumental role in fruit growth and maturation [14]. In addition, the overall repertoire of metabolites in fruits determines their organoleptic properties and functional components.

Essentially comprehensive and nonbiased, metabolomics has emerged as an important discipline for evaluating plant growth and development and involves the untargeted analysis of dynamically catabolized metabolic compounds [15]. In recent years, mass spectrometry (MS)–based metabolomic approaches for the demarcation of the stages of fruit growth and development have been adopted increasingly [16,17]. Enhancement of the sensitivity and precision of high-throughput techniques, such as gas chromatography (GC)–MS, liquid chromatography–mass spectrometry, and capillary electrophoresis–mass spectrometry, has enabled the rapid screening of complex metabolomes [18]. Previously, metabolomic profiling of ginseng plants has substantiated the spatial disparity in metabolite levels between the different plant parts including the roots [19,20]. However, the metabolic changes accompanying the different stages of GB growth and maturity remain largely unknown.

In this study, we used hyphenated MS-based metabolomic methods for delineating the dynamic metabolic events occurring during five different GB maturation stages. Furthermore, we established a correlation between the altered metabolomes and their effects on the functional bioactive compounds in ginseng.

2. Materials and methods

2.1. Chemicals and reagents

HPLC-grade solvents including methanol, acetonitrile, hexane, and water were purchased from Fisher Scientific (Pittsburgh, PA, USA). All standard compounds and analytical grade reagents used in this study were purchased from Sigma-Aldrich (St. Louis, MO, USA).

2.2. Plant materials

GBs in five different stages of development and maturity were harvested from 4-year-old *P. ginseng* plants cultivated in Geumsan County, Chungcheong Province, the Republic of Korea. Different staged berries were harvested at 14, 29, 45, 60, and 76 days after flowering. The five different time points at 15-day intervals were between June and August 2016 (from 03 June 2016 to 04 August 2016), representing the five different maturation stages, namely, immature green (IG): light green fruit collected on the 14th day, mature green (MG): dark green fruit collected on the 29th day, partially red (PR): light red fruit collected on the 45th day, fully red (FR): dark red fruit collected on the 60th day, and overmature (OR): deep brown fruit collected on the 76th day (Fig. 1). GBs are usually harvested when the pericarp color changes from green to red, and therefore, we further classified these five different maturation stages into three broader categories, namely, preharvest (IG and MG), harvest (PR), and postharvest (FR and OR) stages. The freshly harvested GBs were stored under deep-freezing conditions (−20°C) until further analyses. The GBs were freeze-dried for 3 days and homogenized in a blender for metabolite extraction.

2.3. Sample preparation

Each pulverized GB sample (600 mg) was extracted with 6 mL of 70% methanol using a Retsch MM400 mixer mill (Retsch GmbH, Haan, Germany), operated at 30 Hz/s for 10 min. Subsequently, the samples were subjected to sonication in an ultrasonic water bath (Power Sonic 305; Hwashin Technology Co., Seoul, Korea) for 5 min and centrifuged at 17000 rpm at 4°C for 15 min. The supernatant was filtered using a 0.2-μm polytetrafluoroethylene filter and concentrated using a speed vacuum concentrator (Modulspin 31; Biotron, Incheon, Korea). The samples collected finally were weighed and reconstituted in 70% methanol. The final concentration of the samples was 50 mg/mL for ultrahigh performance liquid chromatography–electrospray ionization–tandem mass spectrometry (UHPLC–ESI–MS/MS), ultraperformance liquid chromatography–quadrupole time-of-flight (UPLC–Q-TOF)–MS, and GC–TOF–MS analysis. The samples for GC–TOF–MS analysis were derivatized in a two-step reaction. First, 50 μL of methoxyamine hydrochloride (20 mg/mL in pyridine) was added to the dried samples and heated at 30°C for 90 min. Then, 50 μL of the derivatization agent MSTFA (N-Methyl-N-(trimethylsilyl)trifluoroacetamide) was added to the samples, and the samples were heated at 37°C for 30 min.

The pooled quality control samples were prepared from 50 μL blends of each sample. The analytical samples were analyzed in blocks of 10 runs followed by an intermittent quality control analysis to ensure the data quality and robustness of the method. Three biological replicates and three analytical replicates of each GB sample extract were maintained. Similarly, the sample preparation for antioxidant activity assays involved the previously described extraction procedure.

2.4. GC–TOF–MS analysis

We used an Agilent 7890A GC system (Agilent Technologies, Palo Alto, CA, USA), equipped with an Agilent 7693 autosampler

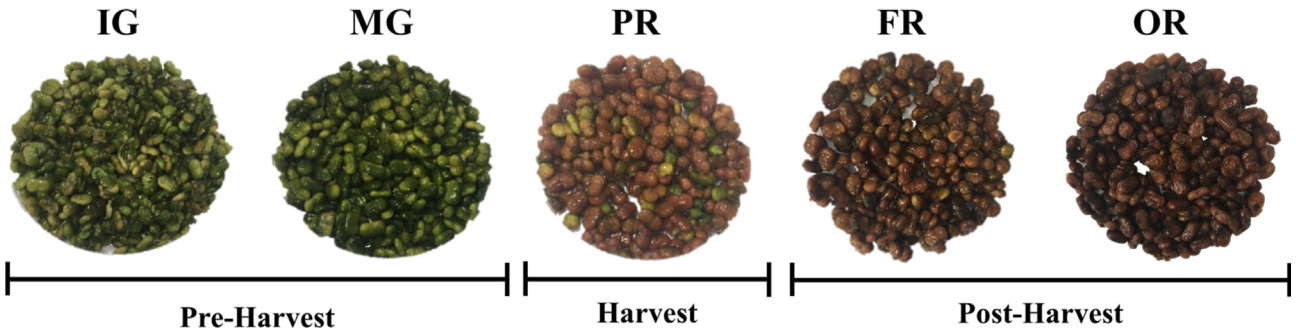

Fig. 1. Different stages of ginseng berry (GB) development and maturation. The morphological changes shown here represent GBs harvested at different stages from the berry of four-year-old *Panax ginseng* Meyer. The five maturation stages were further subdivided into three broader categories depending on usual GB harvest time: preharvest (IG and MG), harvest (PR), and postharvest (FR and OR) stages.
FR, fully red (60 days); IG, immature green (14 days); MG, mature green (29 days); OR, overmature red (76 days); PR, partially red (45 days).

and a TOF Pegasus III mass spectrometer (LECO, St. Joseph, MI, USA) for GC–TOF–MS analysis. Metabolites were separated on an Agilent Rtx-5MS capillary column (J&W Scientific, Folsom, CA, USA) with an internal diameter, film thickness, and length of 0.25 mm, 0.25 μm, and 30 m, respectively. The derivatized samples (1 μL) were injected into the GC–TOF–MS system at a split ratio of 10:1 (v/v). Helium was used as the carrier gas at a constant flow rate of 1.5 mL/min. The injector temperature was maintained at 250°C, whereas the ion source temperature was set at 230°C. The oven temperature was held at 75°C for 2 min, increased to 300°C at a rate of 15°C/min, and then maintained at 300°C for 3 min. The mass acquisition rate was set at 20 scans/s for a mass scan range of 45–1000 *m/z*. The ionization energy for electron ionization was 70 eV.

2.5. UHPLC–ESI–MS/MS and UPLC–Q-TOF–MS analyses

An LTQ XL ion trap mass spectrometer (Thermo Fisher Scientific, San Jose, CA, USA) comprising an electrospray interface coupled with a Dionex UltiMate 3000 RS Pump, RS autosampler, RS column compartment, and RS diode array detector (Dionex Corporation, Sunnyvale, CA, USA) was used in this study. The sample, with an injection volume of 10 μL at a constant flow rate of 0.3 mL/min, was separated on a Thermo Scientific Syncronis C_{18} UHPLC column (100 mm × 2.1 mm [i.d.] × 1.7 μm [particle size]). (Thermo Fisher Scientific, San Jose, CA, USA) The gradient mobile phase consisted of solvent A (water + 0.1% formic acid) and solvent B (acetonitrile + 0.1% formic acid). The LC gradient was increased from 10% solvent B to 100% solvent B in 15 min, maintained for 3 min, and then reequilibrated to the initial condition in 4 min. The photodiode array detector was tuned to a wavelength range of 200–600 nm for metabolite detection, managed by a three-dimensional field. The instrument was operated in a full-scan mode with a mass scan range of 150–1500 *m/z*. The operating parameters were as follows: capillary temperature was 270°C and sheath gas flow and auxiliary gas flow were 40 and 20 arbitrary units, respectively. The conditions in positive ion (and negative ion) mode for ESI were as follows: capillary voltage of 45 kV (−31 kV), source voltage of 5 V (4.5 V), and tube lens voltage of 120 V (−60 V).

UPLC was performed using a Waters Micromass Q-Tof Premier mass spectrometer with an ACQUITY UPLC system (Waters Corporation, Milford, MA, USA), equipped with a Waters ACQUITY UPLC tunable UV detector, autosampler, and binary solvent delivery system. The chromatographic operations were performed using an ACQUITY UPLC BEH C_{18} column (100 mm × 2.1 mm [i.d.] × 1.7 μm [particle size]) (Waters Corporation, Milford, MA, USA) at a flow rate of 0.3 mL/min. The mobile phase comprised water (A) and acetonitrile (B) with 0.1% formic acid (v/v), initially maintained at 5% B for 1 min. The mobile phase gradients were increased from 5% to 100% B over 10 min, maintained at 100% B for 1 min, reduced to 5% B over 2 min, and then, held constant for 1 min. The sample (5 μL) was injected at a constant flow rate of 0.3 mL/min. Mass spectra were recorded in full-spectrum mode over a range of 100–1500 *m/z*. The ion source and desolvation temperatures were set at 100°C and 200°C, respectively, and the desolvation gas flow rate was fixed at 700 L/h. The cone voltage was 40 V and capillary voltage was 2.8 kV in positive ion mode. In negative ion mode, the cone voltage was 60 V, whereas capillary voltage was 2.5 kV.

2.6. Data processing and statistical analysis

The MS raw data files were converted to Network Common Data Form (NetCDF) (*.cdf) format using ChromaTOF (version 4.44, LECO) and Xcalibur software (version 2.2; Thermo Fisher Scientific). After conversion, the NetCDF files were processed using the MetAlign software package (http://www.metalign.nl) to obtain baseline correction, peak alignment, peak detection, accurate masses, and normalized peak intensities [21]. Parameters of MetAlign were set according to the specific scaling requirements and chromatographic and mass spectrometric conditions used in the experiments (Table S1). The resulting data matrix, which contained the sample name and peak area information as variables, was processed using SIMCA-P+ 12.0 (Umetrics, Umea, Sweden) for multivariate statistical analysis. The data sets were log-transformed and UV-scaled before principal component analysis (PCA) and partial least squares discriminant analysis (PLS-DA) modeling. PCA and PLS-DA were performed to compare the different maturation stages of GB. The significantly discriminant metabolite with a variable importance in projection (VIP) value exceeding 1.0 and p value < 0.05 was selected using the PLS-DA model. The p-values for different metabolite-based clusters were determined using Statistica (version 7.0; StatSoft, Tulsa, OK, USA). Variables were detected using MetAlign with the liquid chromatography–mass spectrometry data set.

PASW Statistics 18 (SPSS Inc., Chicago, IL, USA) was used to calculate Pearson's correlation coefficient. The significance of data on total flavonoid content (TFC), total phenolic content (TPC), and antioxidant activity (2,2-azino-bis-(3-ethylbenzothiazoline-6-sulfonic acid) diammonium salt [ABTS] and ferric reducing antioxidant power [FRAP]) was determined using one-way analysis of variance and Duncan's multiple range test using SPSS.

2.7. Identification and visualization of metabolites

The metabolites detected by GC–TOF–MS were putatively identified using standard compounds, an in-house library, and databases of the National Institute of Standards and Technology (NIST MS Search Program, version 2.0, Gaithersburg, MD, USA) by comparing their retention time and mass spectrometry data. Similarly, the metabolites analyzed by UHPLC–ESI–MS/MS were tentatively identified by comparing their retention time, molecular weight, ultraviolet absorption, and MS^n fragment patterns based on standard compounds and published references. Accurate mass and elemental compositions were determined using MassLynx (Waters Corporation) in UPLC-Q-TOF-MS. Variations in the relative abundance of significantly discriminant metabolites among the maturation stages were visualized using a heat map generated using MultiExperiment Viewer (version 4.8.1, http://www.tm4.org/). MultiExperiment Viewer was additionally used to generate correlation heat maps between metabolite levels and antioxidant activity.

2.8. Evaluation of antioxidant activity by ABTS and FRAP assays

The methods of the ABTS free radical scavenging and FRAP assays were adopted from those developed by Lee et al. [11]. All experiments were conducted for the three biological replicates of the GB extracts.

2.9. Determination of TFC and TPC

The TFC and TPC were estimated according to the method described by Lee at al [11]. All experiments were conducted for the three biological replicates of the GB extracts.

3. Results and discussion

3.1. GC–TOF–MS–based primary metabolite profiling for GB extracts

Primary metabolite profiles for the GB extracts across the five different developmental and maturation stages were characterized

by GC–TOF–MS. Multivariate analyses of the aligned datasets indicated a clustered pattern for the extracts of GB under different stages in the PCA (Fig. S1A) and PLS-DA (Fig. 2A) models. Based on the PLS-DA score plot, the patterns of the primary metabolite profiles for the different maturation stages of GB were clustered into three main groups, namely, IG, MG, and three ripened (PR, FR, and OR) stages. The observed satisfaction values of X and Y variables in the PLS-DA model were 0.789 (R^2X) and 0.989 (R^2Y), respectively, with a prediction accuracy of 0.972 (Q^2). Similar patterns were observed in the corresponding PCA (Fig. S1A). The preharvest (IG and MG) stages were separated from the harvest/postharvest (PR, FR, and OR) stages along PLS1 (34.9%), whereas MG was separated from the other four stages along PLS2 (18.2%). Totally, 43 significantly discriminant metabolites, including 16 amino acids and amines, 12 organic acids, 11 sugars and sugar derivatives, and four fatty acids with miscellaneous metabolites, were selected at a VIP value > 1.0 and p value < 0.05 using the PLS-DA model (Table S2). Moreover, the significantly discriminant metabolite variables were indicated in the corresponding loading plots (Fig. 2B), with their relative abundance in the extracts of GB under different stages displayed using the heat map (Fig. 2C).

Under the preharvest stages, the GB extracts exhibited a higher relative abundance of amino acids, specifically alanine (**1**), valine (**2**), isoleucine (**4**), proline (**5**), glycine (**6**), serine (**7**), threonine (**8**), aspartic acid (**9**), pyroglutamic acid (**10**), γ-Aminobutyric acid (GABA) (**11**), phenylalanine (**13**), glutamine (**14**), and lysine (**15**). Reportedly, increased amino acid metabolism in early maturation stages affects fruit development through enhanced respiration, endocarp hardening, phenylpropanoid precursor levels, and aroma compound synthesis [22,23]. Particularly, the higher abundance of serine in the aforementioned ground tissues (leaves, stems, and fruits) is mostly linked with higher rates of photorespiration [24].

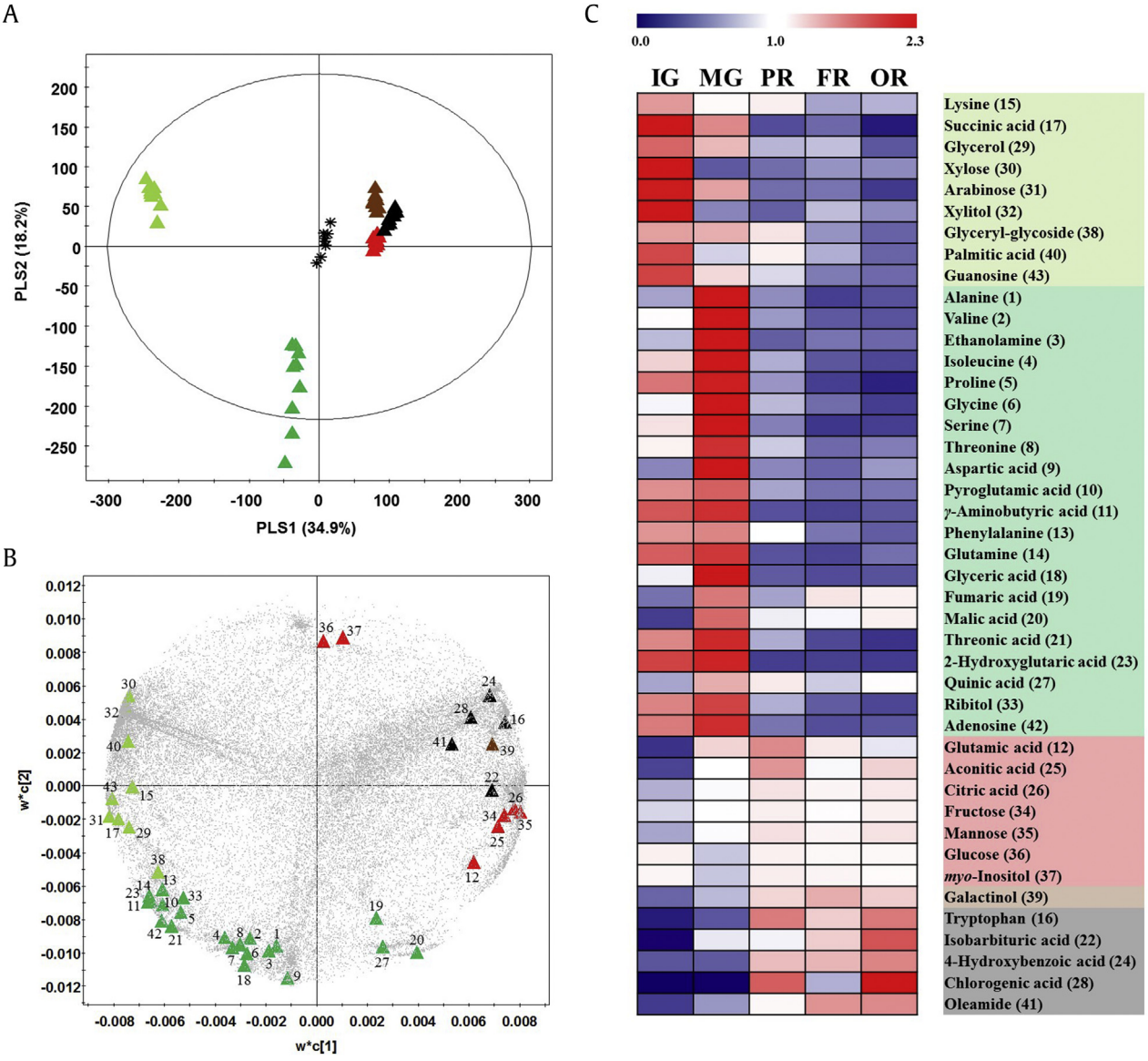

Fig. 2. Multivariate analyses. (A) PLS-DA score plot, (B) loading plot, and (C) heat map showing relative metabolite abundance (average fold change), altogether indicating disparity in primary metabolite contents among GB extracts from different stages, analyzed using GC–TOF–MS datasets. Metabolite numbering is identical to that in Table S2. GB maturation stages are represented by colored triangles in plots A and B: ▲, IG; ▲, MG; ▲, PR; ▲, FR; ▲, OR; *, QC. FR, fully red; GB, ginseng berry; GC–TOF–MS, gas chromatography–time-of-flight–mass spectrometry; IG, immature green; MG, mature green; OR, overmature red; PLS-DA, partial least squares discriminant analysis; GABA, γ-Aminobutyric acid; PR, partially red; QC, quality control.

However, the relative abundance of amino acids decreased during the later stages of GB growth and ripening (Fig. 2C).

Ethanolamine (**3**) levels showed a tendency similar to that of amino acids during the early maturation stages. Biochemically, ethanolamines are synthesized through the decarboxylation of amino acids (mostly serine) and help to promote the overall growth and development of plants [25]. Similarly, the relative abundance of purine nucleosides, such as adenosine (**42**) and guanosine (**43**), were observed to be higher during the preharvest stages of GB development. Nucleosides serve as major energy carriers and the precursors toward the synthesis of nucleotide cofactors and subunits of nucleic acids [26]. Reportedly, high nucleoside levels affect high metabolic fluxes, promoting plant growth and fruit ripening [27]. Therefore, the relatively higher abundance of amino acids, amines, and nucleosides potentially determine higher growth and cell expansion rates, essentially in the early stages of GB development, i.e., IG and MG.

The contents of organic acids in fruits determine their characteristic sour tang, which masks the sweet taste attributed to sugars and certain amino acids [28]. In our study, we observed a distinctive stage-specific pattern of the abundance of organic acids, specifically succinic acid (**17**), glyceric acid (**18**), fumaric acid (**19**), malic acid (**20**), threonic acid (**21**), 2-hydroxyglutaric acid (**23**), and quinic acid (**27**), in the GB extracts. In general, the relative organic acid levels increased linearly until the preharvest stages (IG and MG) and decreased sharply in the subsequent maturation stages. Generally, malic acid occurs as the most abundant organic acid in fruits, acting in conjunction with succinic acid and fumaric acid as the key intermediates of the Krebs cycle, potentially influencing the fruit respiration and ripening [29]. Contrarily, a relatively linear tendency of the levels of certain organic acids, including isobarbituric acid (**22**), 4-hydroxybenzoic acid (**24**), aconitic acid (**25**), citric acid (**26**), and chlorogenic acid (**28**), were observed during the later stages of GB maturation (Fig. 2C). The higher deposition of chlorogenic acid ($\sim$20%) was reportedly linked with the early-stage development of the endosperm and metabolic rerouting to lignin biosynthesis in the later stages concomitant to the temporal maturation of coffee seeds [30]. Hence, we conjectured that phenolic compounds are the specific metabolite biomarkers representing the harvest and postharvest stages of GB maturation (Fig. 2). Functionally, phenolic compounds are known to have potential pharmacological activities against chronic ailments, namely, diabetes, Alzheimer's disease, cancer, and certain bacterial infections [31].

Fruit ripening is characterized by reduced pulp firmness, acidity, and chlorophyll content, coupled with the increased contents of total sugars and aroma volatile compounds [32]. In addition, a balanced quantitative ratio of sugar to organic acid levels is crucial for characterizing the flavor and acidity of fruit pulp [33]. Concerning fruit physiology, the production of sugars via photosynthesis in leaves and their proportional accumulation in fruits mediates the environmental cues governing the growth, development, and maturation of fruits by regulating nutrient response signaling pathways and hormones [34]. In this study, we detected higher relative abundance of xylose (**30**), arabinose (**31**), xylitol (**32**), ribitol (**33**), glycerol (**29**), glyceryl glycoside (**38**), and most 5-carbon sugar derivatives in the preharvest stages than in the harvest/postharvest stages of GB development. Conversely, 6-carbon sugars and their derivatives, including fructose (**34**), mannose (**35**), glucose (**36**), myo-inositol (**37**), and galactinol (**39**), were relatively abundant in the later stages. The enhanced accumulation of sugars and sugar alcohols indicates the higher respiratory needs in plants [24]. Previously, Yamaki and Ino [35] reported that sugar concentrations in fruits are altered variously during maturation and ripening stages. Especially, the high sucrose catabolism during the later stages of fruit development is attributed to the cell wall and vacuolar invertase activity [30]. Considering the organoleptic aspects of fruits, the proportion of different sugars (fructose, glucose, lactose, maltose, sucrose, and trehalose) influencing sweetness is the most important quality trait of fruits, and it is counter-dependent on the ratio of sugar to organic acid levels [36,37]. In GBs, fructose and glucose are the major sugars linked to C3, C6, and C20 of ginsenosides with sugar-binding sites, demonstrated to influence their biological activities including antioxidant activity [38]. Moreover, the high rates of C metabolic pathways provide sufficient energy and C skeleton necessary toward the biosynthesis of ginsenosides [24].

Although a limited number of fatty acids and related compounds were detected in the extracts of GBs harvested at different stages, we observed a reciprocal pattern of the relative levels of 16-C fatty acids (palmitic acid) and the 18-C (unsaturated oleic acid) derivative, i.e., oleamide. Previously, a spatial distinction of the relative distribution of fatty acid compounds was proposed, with palmitic acid (**40**) reportedly accumulating at high levels in leaves and fruits. In olive fruits, unsaturated fatty acid (oleic and linoleic acid) levels increase during ripening, whereas those of saturated fatty acids generally decrease [39]. We observed a relatively higher abundance of oleamide (**41**), an oleic acid derivative, during the later stages of GB maturation. Contrastingly, palmitic acid levels were higher during the preharvest stages and decreased subsequently. Generally, saturated or polyunsaturated fatty acids are synthesized during development, whereas monounsaturated fatty acids are mainly synthesized during fruit growth [40]. Our study revealed a similar pattern during GB maturation, although only two fatty acids were observed to be significantly discriminant.

3.2. *UHPLC–ESI–MS/MS–based secondary metabolite profiling for GB extracts*

Secondary metabolite profiling for the GB extracts representing the different maturation stages was performed by UHPLC–ESI–MS/MS, followed by multivariate analysis of the datasets. As shown in Fig. 3A, the secondary metabolite profiles of the GB extracts exhibited a clustered distribution pattern according to the maturation stage along PLS1 and PLS2, with an overall PLS-DA score plot data variability of 16.7% (PLS1: 11.1% and PLS2: 5.6%). The quality parameters for the PLS-DA model were verified with $R^2X = 0.257$, $R^2Y = 0.993$, and $Q^2Y = 0.849$. The pattern of the secondary metabolite datasets in the PLS-DA model was congruent with the corresponding PCA score plot (Fig. S1B). The datasets for the preharvest stages (IG and MG) were separated from those for the harvest/postharvest stages (PR, FR, and OR) along PLS1, whereas MG and PR were separated from IG, FR, and OR along PLS2. Significantly discriminant secondary metabolites in the GB extracts under different maturation stages were selected at a VIP value > 1.0 and p value < 0.05 using the PLS-DA model. Overall, 24 metabolites, including a phenolic acid, two flavonoids, five notoginsenosides, six ginsenosides, three malonyl (Ma)-ginsenosides, and seven non-identified (NI) metabolites, were selected as significantly discriminant metabolites (Table S3).

The corresponding loading plot for the UHPLC–ESI–MS/MS datasets represented the distribution of the significantly discriminant metabolites along PLS1, signifying these metabolites for the GB maturation stages (Fig. 3B). Excluding ginsenosides Rg1 and Re, most of the ginsenosides were relatively abundant in the preharvest stages. As shown in Fig. 3C, the relative levels of notoginsenoside Fe (**51**), notoginsenoside Fd (**52**), and 20(*S*)-ginsenoside Rg3 (**53**) were higher in the stage IG. However, ginsenoside Rb1 (**47**), Ma-ginsenoside Rb1 (**48**), Ma-ginsenoside Re (**49**), ginsenoside Rd (**50**), notoginsenoside R1 (**54**), Ma-ginsenoside Re (**57**),

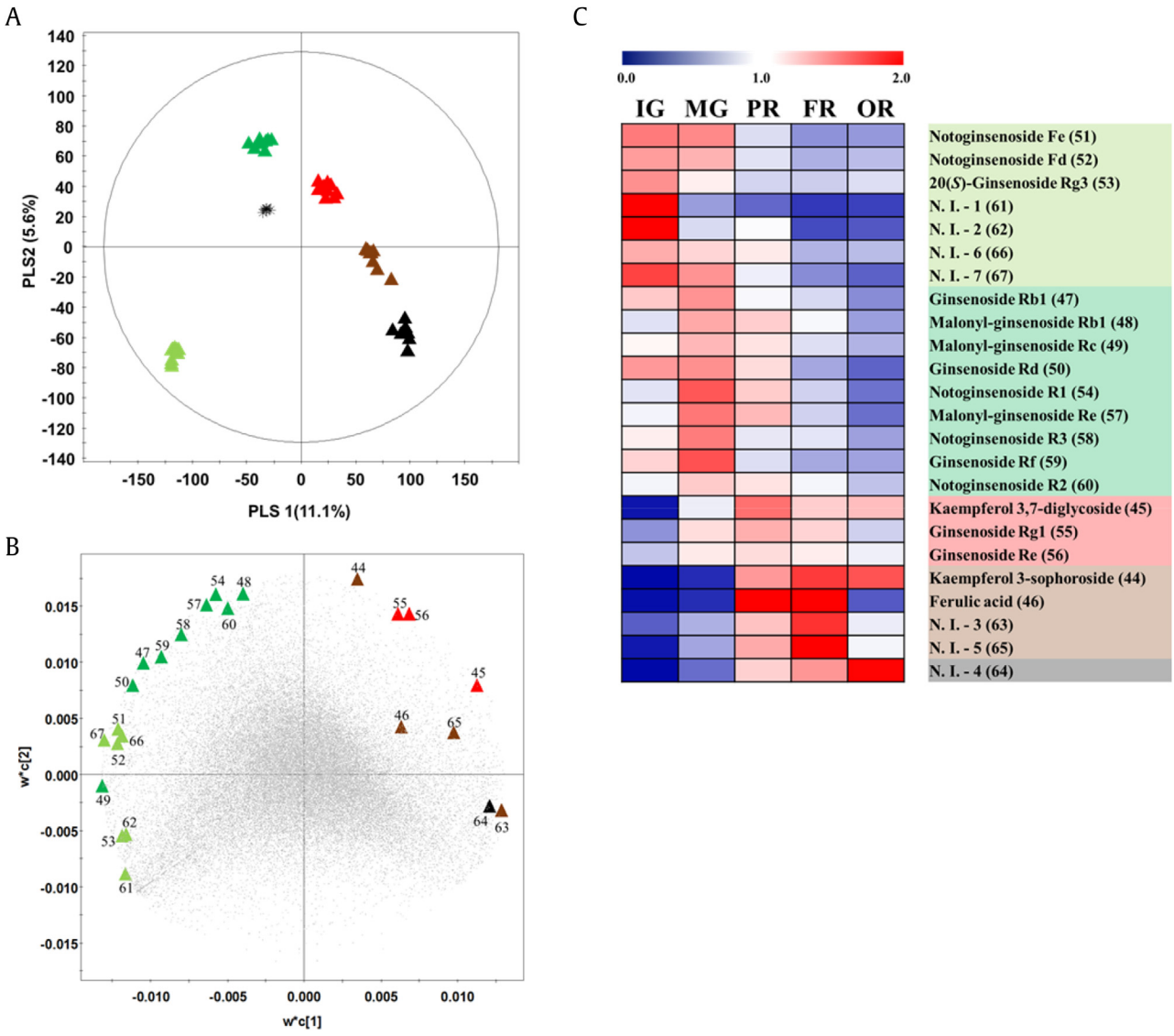

Fig. 3. Multivariate analyses. (A) PLS-DA score plot, (B) loading plot, and (C) heat map showing relative metabolite abundance (average fold change), altogether indicating disparity in secondary metabolite contents among GB extracts from different stages, analyzed using UHPLC–ESI–MS/MS datasets. Metabolite numbering is identical to that in Table S3. GB maturation stages are represented by colored triangles in plots A and B: ▲, IG; ▲, MG; ▲, PR; ▲, FR; ▲, OR; *, QC.
FR, fully red; GB, ginseng berry; IG, immature green; MG, mature green; NI, nonidentified; OR, overmature red; PLS-DA, partial least squares discriminant analysis; PR, partially red; UHPLC–ESI–MS/MS, ultrahigh performance liquid chromatography–electrospray ionization–tandem mass spectrometry; QC, quality control.

notoginsenoside R3 (**58**), ginsenoside Rf (**59**), and notoginsenoside R2 (**60**) were observed to be relatively abundant in the MG stage. Furthermore, the levels of ginsenoside Rg1 (**55**) and ginsenoside Re (**56**) increased gradually until the stage PR and decreased sharply thereafter. Ginsenosides are the active constituents of *P. ginseng*, distributed spatially in its leaves, roots, and berries [41]. The average levels and functional efficacies of ginsenosides, namely, antioxidant, antiinflammatory, antidiabetic, and anticancer components, increase optimally with the plant maturation stage [42,43]. We observed the increased relative abundance of ginsenosides up to the stage MG of GB maturation, followed by a sharp decrease in the subsequent developmental stages. Intriguingly, higher relative abundance of ginsenoside Rg and ginsenoside Rd was observed in the stage PR, which might have contributed to the variance between stages MG and PR along PLS2 in the PLS-DA plot (Fig. 3A). The biosynthesis and accumulation of secondary metabolites in plants is inextricably linked to the transcriptional regulation of genes vital for plant growth and fruit development [44,45]. In agreement with our study, change in fruit color from green to red during ripening results in the marked decrease in saponin levels in holly berries [46]. Similarly, high saponin levels, which reduced considerably on maturation, were detected in unripe *Phytolacca dodecandra* berries [47].

In addition to ginsenosides, the biological and pharmacological properties of *P. ginseng* have been attributed to its phenolic acid contents [48]. The high polyphenol levels in peach, potato, apple, grape, tomato, and ginseng are reported to be related to antitumor, antioxidant, antidiabetic, and cytotoxic activities [49,50]. In addition, ferulic acid, which is present in the plant cell wall as a phenolic phytochemical, has been studied for its antioxidant, antiallergenic, hepatoprotective, and anticarcinogenic activities [51]. Generally, fruit ripening involves a series of complex biochemical reactions resulting in the production of secondary metabolites, such as carotenoids, phenolic compounds, and volatile metabolites [52].

Hence, we proposed that kaempferol 3,7-diglucoside, kaempferol 3-sophoroside, and ferulic acid were synthesized as discriminant metabolites, with relatively higher abundance in the late stages of GB maturation (Fig. 3C). However, the temporal impact of numerous other important factors, including plant nutrition, climatic conditions, and water stress, should be comprehensively studied to understand the metabolic plasticity of GBs under varying maturation stages.

3.3. Analysis of correlation between metabolites in GB extracts and related biochemical phenotypes

We evaluated the antioxidant activities (ABTS and FRAP), TFC, and TPC of the GB extracts representing the different GB maturation stages. As shown in Fig. 4, the antioxidant activities of the extracts of GB in the harvest/postharvest (PR, FR, and OR) stages were relatively higher than those of the preharvest (IG and MG) samples. Although the variations among the late maturation stages were not significantly different, the antioxidant activity determined via the FRAP assay increased markedly at the stage OR compared with the stages PR and FR (Fig. 4B). The TFC and TPC increased linearly as the TFC and TPC activities increased until the late maturation stages. Previously, antioxidant levels in fruits were reported to increase considerably during late maturation stages owing to the increased synthesis and accumulation of antioxidant metabolites [53,54].

A correlation analysis was performed to evaluate the statistical relationship between, altogether, 67 significantly discriminant metabolites and observed tendencies of the related phenotypes, namely, ABTS, FRAP, TFC, and TPC. A correlation map showing both positive (red, $0 < r < 1$) and/or negative (blue, $-1 < r < 0$) correlations was constructed using color-plotted values of normalized variables (Fig. 5). Pearson's correlation coefficients and p-values for all metabolites (60 identified and seven NI metabolites) and corresponding bioactivities are presented in Table S4. Overall, 24 metabolites exhibited positive correlations with the corresponding phenotypes, whereas the remaining 43 showed negative correlations. Interestingly, 29 metabolites with higher relative abundance in the preharvest stage, namely, pyroglutamic acid (**10**), γ-Aminobutyric acid (**11**), succinic acid (**17**), 2-hydroxyglutaric acid (**23**), glycerol (**29**), arabinose (**31**), xylitol (**32**), ribitol (**33**), adenosine (**42**), guanosine (**43**), notoginsenoside Fe (**51**), notoginsenoside Fd (**52**), 20(*S*)-ginsenoside Rg1 (**53**), and three NI metabolites, showed significantly negative correlations ($p < 0.05$) with antioxidant activity. However, the metabolites abundant in the harvest/postharvest stages, specifically tryptophan (**16**), isobarbituric acid (**22**), 4-hydroxybenzoic acid (**24**), aconitic acid (**25**), citric acid (**26**), chlorogenic acid (**28**), fructose (**34**), mannose (**35**), galactinol (**39**), oleamide (**41**), kaempferol 3-sophoroside (**44**), kaempferol 3,7-diglucoside (**45**), and one NI metabolite, showed significantly positive ($p < 0.05$) correlations with antioxidant activity. The metabolites exhibiting positive correlations with

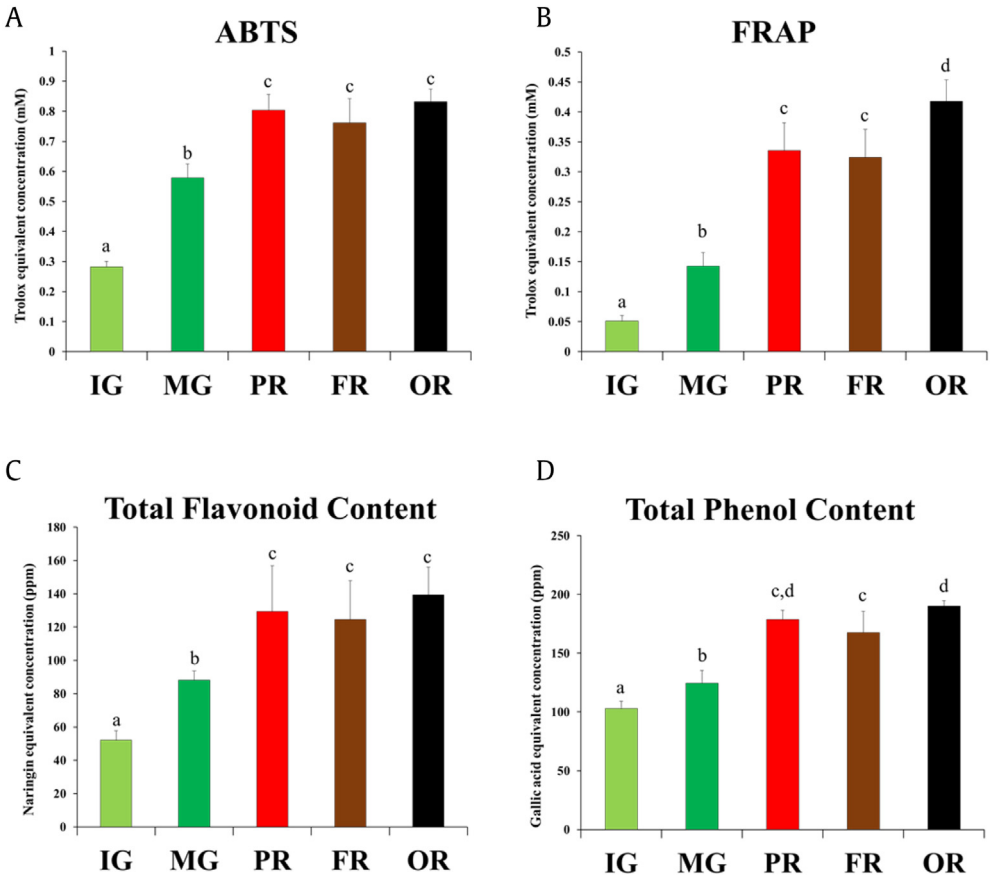

Fig. 4. Antioxidant activity tests. (A) 2,2-azino-bis-(3-ethylbenzothiazoline-6-sulfonic acid) diammonium salt (ABTS), (B) ferric reducing antioxidant power (FRAP), and (C) total flavonoid and (D) total phenolic contents of ginseng berry (GB) extracts from different maturation stages. Here, values are expressed as the average of three biological replicates (n = 3). Bar graphs denoted by the same letter were not significantly different, according to Duncan's multiple range test ($p < 0.05$).
FR, fully red; IG, immature green; MG, mature green; OR, overmature red; PR, partially red.

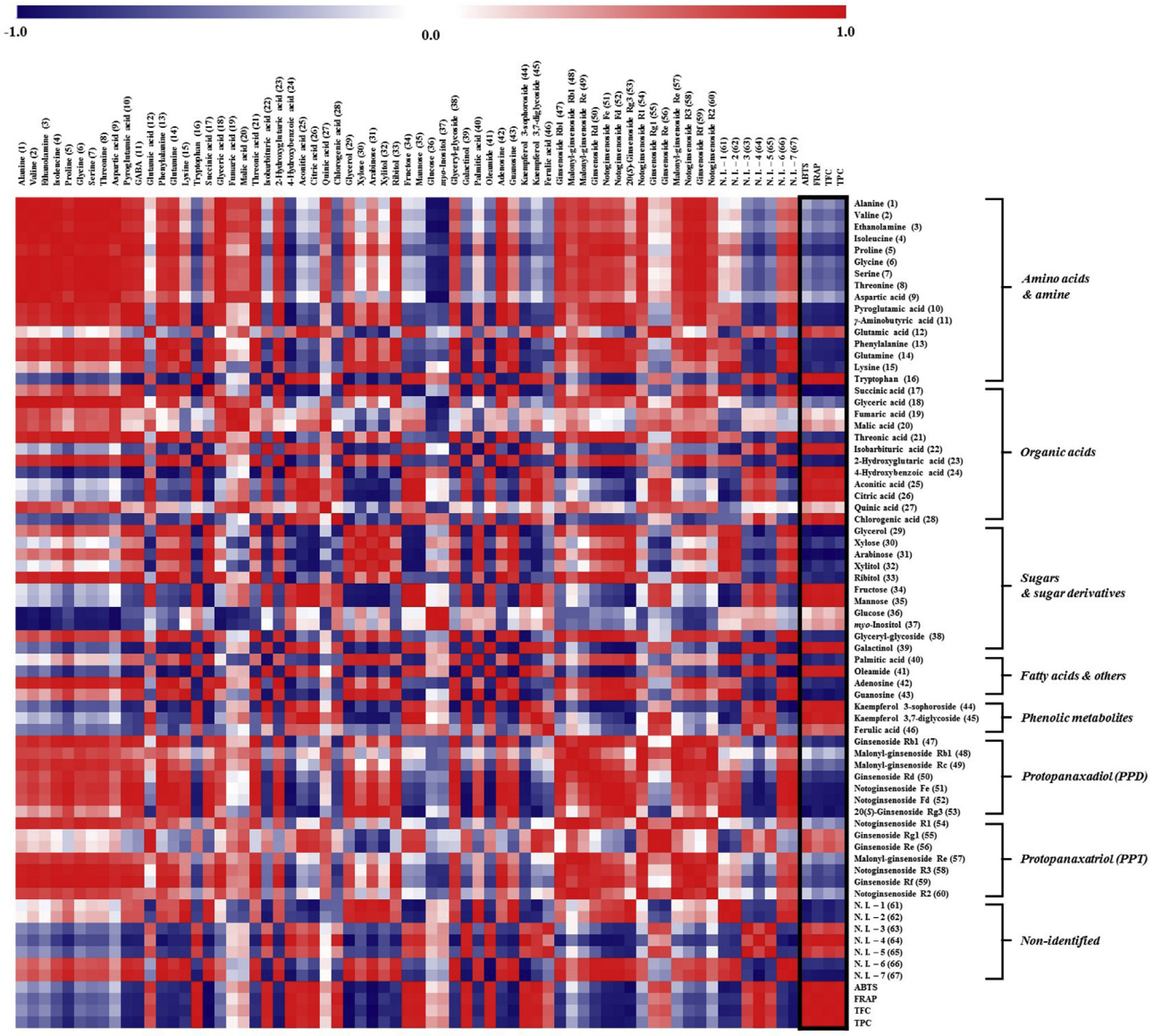

Fig. 5. Heat map representation of correlation analysis between relative abundance of significantly discriminant metabolites and antioxidant activity (ABTS and FRAP), total flavonoid content (TFC) and total phenolic content (TPC) of GB extracts from different maturation stages. Each square indicates Pearson's correlation coefficient values (r). Red and blue represent positive ($0 < r < 1$) and negative ($-1 < r < 0$) correlation, respectively.
ABTS, 2,2-azino-bis-(3-ethylbenzothiazoline-6-sulfonic acid) diammonium salt; FRAP, ferric reducing antioxidant power; GABA, γ-Aminobutyric acid; GB, ginseng berry; NI, nonidentified.

antioxidant activity mainly included phenolic compounds with substantial antioxidant potentials [55]. Typically, 4-hydroxybenzoic acid, chlorogenic acid, kaempferol 3-sophoroside, and kaempferol 3,7-diglucoside are well-studied phenolic compounds in ginseng [48]. However, despite being a phenolic compound, ferulic acid showed weak positive correlations in our study. Previously, chlorogenic acid, kaempferol, and ferulic acid were mainly described as phenolic antioxidants in ginseng with reportedly higher abundance in the fruits [48].

The tendency of phenolic compound levels in the GB extracts increased linearly with maturation stages, especially in OR, characterized morphologically by the deep brown coloration of GBs. Fruit browning is an important biochemical phenomenon influenced by increased polyphenol oxidase activity, causing fruits to soften and darken with deterioration of organoleptic properties [56]. However, this textural transformation negatively affects the flavor, aroma, and overall organoleptic properties of fruits [57]. Hence, optimal fruit maturity is an important agronomic trait as immature fruits lack desirable organoleptic qualities and overmature ones have short shelf lives.

3.4. Scheme of metabolic pathways representing significantly discriminant metabolites among the GBs harvested at different maturation stages

In this study, we examined relevant metabolic pathway maps adopted from the Kyoto Encyclopedia of Genes and Genomes database for more than 60 significantly discriminant primary and secondary metabolites among GBs harvested at different maturation stages. Intriguingly, these metabolites were connected across 10 different pathways, including the citric acid cycle (TCA cycle); glycolysis; pathways of pyrimidine, amino acid, fatty acid, proline, sugar, and purine; ginsenoside metabolism; and shikimate-phenylpropanoid biosynthesis (Fig. 6).

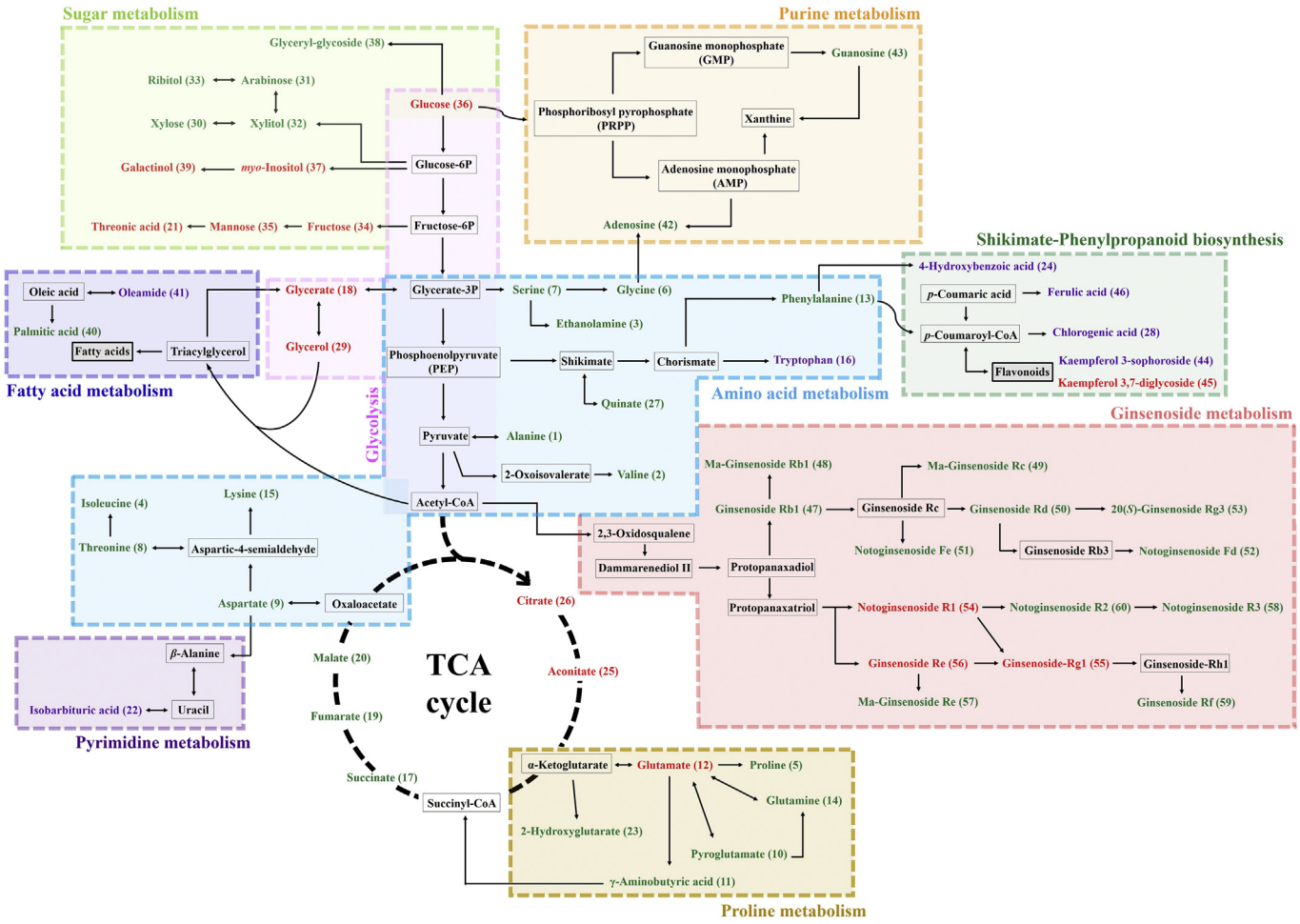

Fig. 6. Schematic representation of pathway maps of significantly discriminant metabolites among GB extracts from different maturation stages. The metabolic pathway scheme was adapted from the KEGG database (http://www.genome.jp/kegg/). Each text color indicates a significantly discriminant metabolite with higher abundance in a particular maturation stage of GB; green: preharvest stages (IG and MG), red: harvest stage (PR), and purple: postharvest stages (FR and OR). Metabolites shown in black boxes were not detected in this study.

ATP, Adenosine triphosphate; NADH, Nicotinamide adenine dinucleotide reduced FR, fully red; GABA, γ-Aminobutyric acid; GB, ginseng berry; IG, immature green; KEGG, Kyoto Encyclopedia of Genes and Genomes; MG, mature green; OR, overmature red; PR, partially red; TCA cycle, citric acid cycle.

Carbon metabolism primarily affects the bioenergetics of organisms and provides C skeletons for the synthesis of complex biomolecules regulating growth, development, and metabolism. In plants, C metabolic pathways, namely, the TCA cycle, glycolysis, sugar metabolism, and shikimate-phenylpropanoid biosynthesis, are chiefly related to plant growth and senescence and regulate plant physiological processes [58]. Changes in metabolite levels in different GB maturation stages were accompanied by an alteration in carbohydrate metabolism, especially glycolysis and the TCA cycle, which play central roles in determining the final metabolite composition in berries [59]. Sucrose and its interconversion into glucose and fructose, with numerous intermediates, feed the TCA cycle and glycolysis, generating energy molecules and reducing power sources, such as Adenosine triphosphate (ATP) and Nicotinamide adenine dinucleotide reduced (NADH) [60]. Together with amino acids and organic acids, these sugars constitute the energy source combining both photosynthesis and respiration in plants [61]. Glycolysis is the first step in the degradation of glucose to ATP, simultaneously generating precursors for the synthesis of organic acids, amino acids, anthocyanins, and numerous other secondary metabolites, including aroma compounds [62]. Reportedly, accumulated organic acids promote fruit ripening by affecting amino acid catabolism, essential for fruit maturation [63]. In our study, the preharvest stages, involving the transformation of GBs from IG to MG, include size increase and pericarp color changes (Fig. 1). These maturation stages showed high abundance of metabolite precursors for glycolysis and the TCA cycle.

Furthermore, shikimate-phenylpropanoid pathways provide alternative ways for aromatic compound synthesis, resulting in the biosynthesis of aromatic amino acids, including tyrosine, phenylalanine, and tryptophan [64]. In the preharvest GB extracts, we detected relatively higher phenylalanine levels, which decreased sharply in the later stages. Functionally, this generates several antioxidants (flavonoids, lignins, and phenols) and their precursors (aromatic amino acids and shikimic acid), which inhibit the activities of reactive oxygen species in plants and protect cell proteins, membrane lipids, and nucleic acids from ensuing damage [65]. The alkaloids and phenolic compounds derived from aromatic amino acids perform similar physiological functions.

The characteristic functional metabolites in GBs, i.e., ginsenosides, are a class of tetracyclic triterpenoid saponins, synthesized via dammarenediol-II hydroxylation by the Cyt P450 enzymes, followed by a glycosylation step catalyzed by glycosyltransferases [66]. Consequently, after the addition of monosaccharides to triterpene aglycones by glycosyltransferases, diverse ginsenosides are produced [67]. In our study, we detected 15 ginsenosides,

including protopanaxadiol and protopanaxatriol types, with most of them showing higher abundance during the preharvest stages. Saponin levels in plants are reportedly influenced by the surrounding environment and growth and development stages [68]. Moreover, progressive increase in oxidative stress during fruit development due to reduced activities of antioxidant enzymes, namely, superoxide dismutase, lipoxygenase, and catalase, potentially favors antioxidant accumulation [69]. Hence, we inferred that the observed higher relative ginsenoside levels in the preharvest stages were related to the ripening and maturation of GB.

Moreover, we observed higher abundance of phenolic compounds derived from the shikimate-phenylpropanoid pathway in the harvest/postharvest (PR, FR, and OR)-staged extracts of GBs. These metabolites were verified to be significantly discriminant in the later stages and correlated positively with synchronous antioxidant activity. Considering metabolites to be more generic markers than the corresponding species-specific transcripts, we conjectured about the conserved metabolic pathways potentially influencing berry maturation across different ginseng species.

4. Conclusion

We assert that the metabolome of the GBs varies markedly at different maturation stages, accompanying its biomolecular, physiological, and morphological condition, which in turn regulates its organoleptic and functional properties. Notably, we demonstrated that C metabolism–related metabolites (organic acids and 5-C sugars) and most ginsenosides were abundant during the preharvest stages, i.e., IG and MG. However, antioxidant metabolites, i.e., flavonoids and phenolic compounds, accumulated at higher levels in the later harvest/postharvest (PR, FR and OR) stages of GB maturation. Therefore, we assume that detailed understanding of maturation stage–related metabolic tendency and related phenotypes of GBs would provide a metabolomic “snapshot” of the subtle transcriptomic–metabolomic networks governing the agro-economic traits and market values of GBs.

Conflicts of interest

The authors declare no conflict of interest.

Acknowledgments

This work was supported by a grant from the Next-Generation BioGreen 21 Program (grant No. PJ01334603), Rural Development Administration, the Republic of Korea. This work was also supported by the Korea Institute of Planning and Evaluation for Technology in Food, Agriculture and Forestry (IPET) through the Agricultural Microbiome R&D Program (Strategic Initiative for Microbiomes in Agriculture and Food), funded by the Ministry of Agriculture, Food and Rural Affairs (Grant number 918011-04-1-HD020).

Appendix A. Supplementary data

Supplementary data to this article can be found online at https://doi.org/10.1016/j.jgr.2019.02.002.

References

[1] Choi J, Kim TH, Choi TY, Lee MS. Ginseng for health care: a systematic review of randomized controlled trials in Korean literature. PLoS One 2013;8:1–14.
[2] Kim YJ, Jeon JN, Jang MG, Oh JY, Kwon WS, Jung SK, Yang DC. Ginsenoside profiles and related gene expression during foliation in *Panax ginseng* Meyer. J Ginseng Res 2014;38:66–72.
[3] Qi LW, Wang CZ, Yuan CS. Ginsenosides from American ginseng: chemical and pharmacological diversity. Phytochemistry 2011;72:689–99.
[4] Chen S, Luo H, Li Y, Sun Y, Wu Q, Niu Y, Song J, Lv A, Zhu Y, Sun C, et al. 454 EST analysis detects genes putatively involved in ginsenoside biosynthesis in *Panax ginseng*. Plant Cell Rep 2011;30:1593–601.
[5] Yuan CS, Wang CZ, Wicks SM, Qi LW. Chemical and pharmacological studies of saponins with a focus on American ginseng. J Ginseng Res 2010;34:160–7.
[6] Oh JY, Kim YJ, Jang MG, Joo SC, Kwon WS, Kim SY, Jung SK, Yang DC. Investigation of ginsenosides in different tissues after elicitor treatment in *Panax ginseng*. J Ginseng Res 2014;38:270–7.
[7] Jiménez Z, Kim YJ, Mathiyalagan R, Seo KH, Mohanan P, Ahn JC, Kim YJ, Yang DC. Assessment of radical scavenging, whitening and moisture retention activities of *Panax ginseng* berry mediated gold nanoparticles as safe and efficient novel cosmetic material. Artif Cells Nanomed Biotechnol 2017;9:1–8.
[8] Zhang W, Cho SY, Xiang G, Min KJ, Yu Q, Jin JO. Ginseng berry extract promotes maturation of mouse dendritic cells. PLoS One 2015;10:1–14.
[9] Xie JT, Zhou YP, Dey L, Attele AS, Wu JA, Gu M, Polonsky KS, Yuan CS. Ginseng berry reduces blood glucose and body weight in db/db mice. Phytomedicine 2000;9:254–8.
[10] Wang CZ, Zhang B, Song WX, Wang A, Ni M, Luo X, Aung HH, Xie JT, Tong R, He TC, al at. Steamed American ginseng berry: ginsenoside analyses and anticancer activities. J Agric Food Chem 2006;54:9936–42.
[11] Lee MY, Singh D, Kim SH, Lee SJ, Lee CH. Ultrahigh pressure processing produces alterations in the metabolite profiles of *Panax ginseng*. Molecules 2016;21:1–16.
[12] Kim YK, Yoo DS, Xu H, Park NI, Kim HH, Choi JE, Park SU. Ginsenoside content of berries and roots of three typical Korean ginseng (*Panax ginseng*) cultivars. Nat Prod Commun 2009;4:903–6.
[13] Srivastava A, Gupta AK, Datsenka T, Mattoo AK, Handa AK. Maturity and ripening-stage specific modulation of tomato (*Solanum lycopersicum*) fruit transcriptome. GM Crops 2010;1:237–49.
[14] Wang HP, Liu Y, Chen C, Xiao HB. Screening specific biomarkers of herbs using a metabolomics approach: a case study of *Panax ginseng*. Sci Rep 2017;7:1–9.
[15] Tarpley L, Duran AL, Kebrom TH, Sumner LW. Biomarker metabolites capturing the metabolite variance present in a rice plant developmental period. BMC Plant Biol 2005;5:1–12.
[16] White IR, Blake RS, Taylor AJ, Monks PS. Metabolite profiling of the ripening of Mangoes *Mangifera indica* L. cv. 'Tommy Atkins' by real-time measurement of volatile organic compounds. Metabolomics 2016;12:1–11.
[17] Diboun I, Mathew S, Al-Rayyashi M, Elrayess M, Torres M, Halama A, Méret M, Mohney RP, Karoly ED, Malek J, al at. Metabolomics of dates (*Phoenix dactylifera*) reveals a highly dynamic ripening process accounting for major variation in fruit composition. BMC Plant Biol 2015;15:1–22.
[18] Lisec J, Schauer N, Kopka J, Willmitzer L, Fernie AR. Gas chromatography mass spectrometry-based metabolite profiling in plants. Nat Protoc 2006;1:387–96.
[19] Yang SO, Shin YS, Hyun SH, Cho S, Bang KH, Lee D, Choi SP, Choi HK. NMR-based metabolic profiling and differentiation of ginseng roots according to cultivation ages. J Pharm Biomed Anal 2012;58:19–26.
[20] Wang JR, Yau LF, Gao WN, Liu Y, Yick PW, Liu L, Jiang ZH. Quantitative comparison and metabolite profiling of saponins in different parts of the root of *Panax notoginseng*. J Agric Food Chem 2014;62:9024–34.
[21] Lommen A, Kools HJ. MetAlign 3.0: performance enhancement by efficient use of advances in computer hardware. Metabolomic 2012;8:719–26.
[22] Lombardo VA, Osorio S, Borsani J, Lauxmann MA, Bustamante CA, Budde CO, Andreo CS, Lara MV, Fernie AR, Drincovich MF. Metabolic profiling during peach fruit development and ripening reveals the metabolic networks that underpin each developmental stage. Plant Physiol 2011;157:1696–710.
[23] Lamikanra O, Kassa AK. Changes in the free amino acid composition with maturity of the noble cultivar of *Vitis rotundifolia Michx*. grape. J Agric Food Chem 1999;47:4837–41.
[24] Liu J, Liu Y, Wang Y, Abozeid A, Zu YG, Tang ZH. The integration of GC-MS and LC-MS to assay the metabolomics profiling in *Panax ginseng* and *Panax quinquefolius* reveals a tissue- and species-specific connectivity of primary metabolites and ginsenosides accumulation. J Pharm Biomed Anal 2017;135:176–85.
[25] Rontein D, Nishida I, Tashiro G, Yoshioka K, Wu WI, Voelker DR, Basset G, Hanson AD. Plants synthesize ethanolamine by direct decarboxylation of serine using a pyridoxal phosphate enzyme. J Biol Chem 2001;276:35523–9.
[26] Moffatt BA, Ashihara H. Purine and pyrimidine nucleotide synthesis and metabolism. Arabidopsis Book 2002;1:e0018.
[27] Colombié S, Nazaret C, Bénard C, Biais B, Mengin V, Solé M, Fouillen L, Dieuaide-Noubhani M, Mazat J, Beauvoit B, et al. Modelling central metabolic fluxes by constraint-based optimization reveals metabolic reprogramming of developing *Solanum lycopersicum* (tomato) fruit. Plant J 2015;81:24–39.
[28] Lobit P, Genard M, Soing P, Habib R. Modelling malic acid accumulation in fruits: relationships with organic acids, potassium, and temperature. J Exp Bot 2006;57:1471–83.
[29] Merchante C, Vallarino JG, Osorio S, Aragüez I, Villarreal N, Ariza MT, Martínez GA, Medina-Escobar N, Civello MP, Fernie AR, et al. Ethylene is involved in strawberry fruit ripening in an organ-specific manner. J Exp Bot 2013;64:4421–39.

[30] Joët T, Laffargue A, Salmona J, Doulbeau S, Descroix F, Bertrand B, de Kochko A, Dussert S. Metabolic pathways in tropical dicotyledonous albuminous seeds: *Coffea arabica* as a case study. New Phytol 2009;182:146–62.
[31] Spilioti E, Jaakkola M, Tolonen T, Lipponen M, Virtanen V, Chinou I, Kassi E, Karabournioti S, Moutsatsou P. Phenolic acid composition, antiatherogenic and anticancer potential of honeys derived from various regions in Greece. PLoS One 2014;9:1–10.
[32] Yashoda HM, Prabha TN, Tharanathan RN. Mango ripening: changes in cell wall constituents in relation to textural softening. J Sci Food Agric 2008;86: 713–21.
[33] Sweetman C, Sadras VO, Hancock RD, Soole KL, Ford CM. Metabolic effects of elevated temperature on organic acid degradation in ripening *Vitis vinifera* fruit. J Exp Bot 2014;65:5975–88.
[34] Rolland F, Baena-Gonzalez E, Sheen J. Sugar sensing and signaling in plants: conserved and novel mechanisms. Annu Rev Plant Biol 2006;57:675–709.
[35] Yamaki S, Ino M. Alteration of cellular compartmentation and membrane permeability to sugars in immature and mature apple fruit. JASHS 1992;117: 951–4.
[36] Nardozza S, Boldingh HL, Osorio S, Höhne M, Wohlers M, Gleave AP, MacRae EA, Richardson AC, Atkinson RG, Sulpice R, et al. Metabolic analysis of kiwifruit (*Actinidia deliciosa*) berries from extreme genotypes reveals hallmarks for fruit starch metabolism. J Exp Bot 2013;64:5049–63.
[37] Clemens RA, Jones JM, Kern M, Lee S-Y, Mayhew EJ, Slavin JL, Zivanovic S. Functionality of sugars in foods and health. Compr Rev Food Sci Food Saf 2016;15:433–70.
[38] Jee HS, Chang KH, Park SH, Kim KT, Paik HD. Morphological characterization, chemical components, and biofunctional activities of *Panax ginseng, Panax quinquefolium*, and *Panax notoginseng* roots: a Comparative Study. Food Rev Int 2014;30:91–111.
[39] Beltrán G, Del Rio C, Sánchez S, Martínez L. Influence of harvest date and crop yield on the fatty acid composition of virgin olive oils from cv. Picual. J Agric Food Chem 2004;52:3434–40.
[40] Mazilak P. Lipids. In: Hulme AC, editor. The biochemistry of fruits and their products. New York: Academic Press; 1970. p. 209–38.
[41] Attele AS, Wu JA, Yuan CS. Ginseng pharmacology: multiple constituents and multiple actions. Biochem Pharmacol 1999;58:1685–93.
[42] Attele AS, Zhou YP, Xie JT, Wu JA, Zhang L, Dey L, Pugh W, Rue PA, Polonsky KS, Yuan CS. Antidiabetic effects of *Panax ginseng* berry extract and the identification of an effective component. Diabetes 2002;51:1851–8.
[43] Soldati F, Tanaka O. *Panax ginseng*: relation between age of plant and content of ginsenosides. Planta Med 1984;50:351–2.
[44] Han JY, In JG, Kwon YS, Choi YE. Regulation of ginsenoside and phytosterol biosynthesis by RNA interferences of squalene epoxidase gene in *Panax ginseng*. Phytochemistry 2010;71:36–46.
[45] Kim OT, Kim SH, Ohyama K, Muranaka T, Choi YE, Lee HY, Kim MY, Hwang B. Upregulation of phytosterol and triterpene biosynthesis in *Centella asiatica* hairy roots overexpressed ginseng farnesyl diphosphate synthase. Plant Cell Rep 2010;4:403–11.
[46] Kreuger B, Potter DA. Changes in saponins and tannins in ripening holly Fruits and effects of fruit consumption on nonadapted insect herbivores. Am Midl Nat 1994;132:183–91.
[47] Ndamba J, Lemmich E, Mølgaard P. Investigation of the diurnal, ontogenetic and seasonal variation in the molluscicidal saponin content of *Phytolacca dodecandra* aqueous berry extracts. Phytochemistry 1994;35:95–9.
[48] Chung IM, Lim JJ, Ahn MS, Jeong HN, An TJ, Kim S. Comparative phenolic compound profiles and antioxidative activity of the fruit, leaves, and roots of Korean ginseng (*Panax ginseng* Meyer) according to cultivation years. J Ginseng Res 2016;40:68–75.
[49] Brito A, Ramirez JE, Areche C, Sepúlveda B, Simirgiotis MJ. HPLC-UV-MS profiles of phenolic compounds and antioxidant activity of fruits from three citrus species consumed in Northern Chile. Molecules 2014;19: 17400–21.
[50] Kim TH, Ku SK, Lee IC, Bae JS. Anti-inflammatory effects of kaempferol-3-O-sophoroside in human endothelial cells. Inflamm Res 2012;61:217–24.
[51] Kumar N, Pruthi V. Potential applications of ferulic acid from natural sources. Biotechnol Rep (Amst) 2014;4:86–93.
[52] Theologis A, Zarembinski T, Oeller PW, Liang X, Abel S. Modification of fruit ripening by suppressing gene expression. Plant Physiol 1992;100:549–51.
[53] Shin GR, Lee S, Lee S, Do SG, Shin E, Lee CH. Maturity stage-specific metabolite profiling of *Cudrania tricuspidata* and its correlation with antioxidant activity. Ind Crops Prod 2015;70:322–31.
[54] Çelik H, Özgen M, Serçe S, Kaya C. Phytochemical accumulation and antioxidant capacity at four maturity stages of cranberry fruit. Sci Hortic 2008;117: 345–8.
[55] Balasundram N, Sundram K, Samman S. Phenolic compounds in plants and agri-industrial by-products: antioxidant activity, occurrence, and potential uses. Food Chem 2006;99:191–203.
[56] Altunkaya A, Gökmen V. Effect of various inhibitors on enzymatic browning, antioxidant activity and total phenol content of fresh lettuce (*Lactuca sativa*). Food Chem 2008;170:1173–9.
[57] Holderbaum DF, Kon T, kudo T, Guerra MP. Enzymatic browning, polyphenol oxidase activity, and polyphenols in four apple cultivars: dynamics during fruit development. Hortscience 2010;45:1150–4.
[58] Zhao Y, Zhao J, Zhao C, Zhou H, Li Y, Zhang J, Li L, Hu C, Li W, Peng X, et al. A metabolomics study delineating geographical location-associated primary metabolic changes in the leaves of growing tobacco plants by GC-MS and CE-MS. Sci Rep 2015;5:1–11.
[59] Dai ZW, Léon C, Feil R, Lunn JE, Delrot S, Gomès E. Metabolic profiling reveals coordinated switches in primary carbohydrate metabolism in grape berry (*Vitis vinifera* L.), a non-climacteric fleshy fruit. J Exp Bot 2013;64:1345–55.
[60] Sturm A. Primary structures, functions, and roles in plant development and sucrose partitioning. Plant Physiol 1999;121:1–8.
[61] Lee S, Do SG, Kim SY, Kim J, Jin Y, Lee CH. Mass spectrometry-based metabolite profiling and antioxidant activity of Aloe vera (*Aloe barbadensis* Miller) in different growth stages. J Agric Food Chem 2012;60:11222–8.
[62] Crowhurst RN, Gleave AP, MacRae EA, Ampomah-Dwamena C, Atkinson RG, Beuning LL, Bulley SM, Chagne D, Marsh KB, Matich AJ, al at. Analysis of expressed sequence tags from *Actinidia*: applications of a cross species EST database for gene discovery in the areas of flavor, health, color and ripening. BMC Genomics 2008;9:1–26.
[63] Rocco M, D'Ambrosio C, Arena S, Faurobert M, Scaloni A, Marra M. Proteomic analysis of tomato fruits from two ecotypes during ripening. Proteomics 2006;6:3781–91.
[64] Tzin V, Galili G. The biosynthetic pathways for shikimate and aromatic amino acids in Arabidopsis thaliana. Arabidopsis Book 2010;8:1–18.
[65] Dixon RA, Achnine L, Kota P, Liu CJ, Reddy MS, Wang L. The phenylpropanoid pathway and plant defence-a genomics perspective. Mol Plant Pathol 2002;3: 371–90.
[66] Shibuya M, Hoshino M, Katsube Y, Hayashi H, Kushiro T, Ebizuka Y. Identification of beta-amyrin and sophoradiol 24-hydroxylase by expressed sequence tag mining and functional expression assay. FEBS J 2006;273:948–59.
[67] Choi DW, Jung J, Ha Y, Park HW, In DS, Chung HJ, Liu JR. Analysis of transcripts in methyl jasmonate-treated ginseng hairy roots to identify genes involved in the biosynthesis of ginsenosides and other secondary metabolites. Plant Cell Rep 2005;23:557–66.
[68] Moses T, Papadopoulou KK, Osbourn A. Metabolic and functional diversity of saponins, biosynthetic intermediates and semi-synthetic derivatives. Crit Rev Biochem Mol Biol 2014;49:439–62.
[69] Mondal K, Sharma NS, Malhotra SP, Dhawan K, Singh R. Antioxidant systems in ripening tomato fruits. Biologia Plantarum 2004;48:49–53.